International Journal of Innovative
Computing, Information and Control
Volume **16**, Number **2**, April **2020**

ICIC International ©2020 ISSN 1349-4198
pp. 715–732

TWO-DEGREE-OF-FREEDOM PIDA CONTROLLERS DESIGN OPTIMIZATION FOR LIQUID-LEVEL SYSTEM BY USING MODIFIED BAT ALGORITHM

Kittisak Lurang and Deacha Puangdownreong

Department of Electrical Engineering
Southeast Asia University
19/1 Petchkasem Road, Nongkhangphlu, Nonghkaem, Bangkok 10160, Thailand
deachap@sau.ac.th

Received August 2019; revised December 2019

Abstract. *In this paper, an optimal design of the two-degree-of-freedom proportional-integral-derivative-accelerated (2DOF-PIDA) controllers for the liquid-level system based on the modern optimization by using the modified bat algorithm (MBA) is proposed. The MBA is the new modified version of the original bat algorithm (BA) developed from the echolocation behaviour of microbats. To improve its exploration and exploitation properties, the random number drawn from a Lévy-flight distribution and new loudness and pulse emission rate functions are proposed. Performance of the MBA over the BA investigated against 10 benchmark functions is presented in this paper. Results of the 2DOF-PIDA controllers designed by the proposed MBA for the liquid-level system are compared with those of the one-degree-of-freedom proportional-integral-derivative (1DOF-PID) controller designed by Ziegler-Nichols (ZN) tuning rule, 2DOF-PID designed by Araki-Taguchi (AT) tuning rule and 1DOF-PID and 1DOF-PIDA controllers designed by the MBA. As results, it was found that the liquid-level controlled system with the 2DOF-PIDA controllers designed by the MBA can provide very satisfactory responses superior to that with the 2DOF-PID controllers designed by AT and MBA and 1DOF-PID controller designed by ZN, significantly.*

Keywords: 2DOF-PIDA controllers, Modified bat algorithm, Liquid-level system, Modern optimization

1. **Introduction.** Traditionally, the 1DOF control system has been widely conducted due to ease of use and simple realization. However, the design of control system which depends on two main purposes, i.e., input-tracking (or command-following) and load-regulating (or disturbance-rejecting), needs to be achieved [1-3]. The 1DOF control system can serve only one purpose. For the 1DOF control system, if the input-tracking response is good, its load-regulating response is poor, and vice versa. This is one of the most significant problems of control practical which most researchers tend to ignore. In control theory, the degree-of-freedom of a control system can be defined by the number of control loops that can be adjusted independently [4-6]. On the other hand, the degree-of-freedom of a control system refers to how many of these closed-loop transfer functions are independent. Due to this, the 2DOF control system has advantages over the 1DOF control system in order to serve both two main purposes of control system design [4-6]. The 2DOF control system has been launched since the mid-19th century [4] and the 2DOF-PID controllers were analyzed and proposed for industrial uses [7-9]. Consequently, the results obtained by the 2DOF-PID controllers were reported [10,11]. Extended studies of 2DOF-PID controllers were conducted for optimal analytical tuning

DOI: 10.24507/ijicic.16.02.715

[12-14], digital 2DOF-PID controllers implementation with magnitude and slope limiters [15] and other 2DOF-PID topics in industrial applications [16-18].

Over two decades, control design paradigm has been changed from conventional analytical approach to new framework by using the metaheuristic optimization approach [19]. Metaheuristic optimization has become potential candidates and widely applied to various engineering problems. Such the metaheuristic optimization techniques have been increasingly applied to optimal tuning of the 2DOF-PID controllers, for example, immune algorithm (IA) for parallel distributed network [20], evolutionary computing (EC) for systems with time-delay [21], genetic algorithm (GA) for first order plus dead time (FOPDT) system [22], bacterial foraging (BF) for unstable systems [23], cuckoo search (CS) and firefly algorithm (FA) for automatic generation control [24], GA for discrete system [25] and the 2DOF-PID controllers of brushless DC motor speed control by current search (CuS) [26].

In 2012, the bat-inspired algorithm (or shortly bat algorithm: BA) was firstly proposed by Yang as one of the most efficient bio-inspired population-based metaheuristic optimization searching techniques [27]. Based on the echolocation or bio-sonar characteristics of microbats, these bats can find their prey and discriminate different types of insects even in complete darkness. The BA developed by Yang [27,28] is based on such the echolocation behavior. The BA has been successfully applied to solving many engineering problems, for instance, welded beam design, pressure vessel design, car side design, spring design, truss system design, series-parallel power system optimization, brushless DC wheel motor design, economic load and emission dispatch optimization, scheduling, image processing, and control systems. Motivation and various applications of the BA have been reviewed and reported [29-31].

Although, the original BA has been accepted for various optimization problems because of its good exploitation property, it has a poor exploration property. The original BA is usually unable to release the search moving from a local entrapment. This problem has been overcome by different modifications made to the original BA. These include the fuzzy logic bat algorithm (FLBA) [32], multiobjective bat algorithm (MOBA) [28], K-means bat algorithm (KMBA) [33], chaotic bat algorithm (CBA) [34], binary bat algorithm (BBA) [35], differential operator and Lévy fights bat algorithm (DLBA) [36], mutation-based bat algorithm [37], hybrid bat algorithm (HBA) [38] and modified bat algorithm (mBA) [39].

In this paper, the modified bat algorithm (MBA) is proposed to improve the performance of the original BA. In the algorithm of the proposed MBA, the random number drawn from a Lévy-flight distribution and new loudness and pulse emission rate functions are proposed to improve its exploration and exploitation properties. The proposed MBA and the mBA [39] are not the same. This is because the mBA [39] uses elite opposition-based learning (EOBL) with the uniformly random number to diversify the solution and the inertial weight to improve its exploitation, while the proposed MBA utilizes the random number with a Lévy-flight distribution to improve its diversification and new loudness and pulse emission rate functions to improve its exploitation. In addition, the proposed MBA may resemble the DLBA [36] in that both DLBA and proposed MBA utilize the random number with a Lévy-flight distribution. However, the DLBA [36] uses differential operator which can provide very quick convergence, but it is usually unable to escape from a local entrapment.

The proportional-integral-derivative-accelerated (PIDA) controller was firstly proposed by Jung and Dorf in 1996 [40]. With its three arbitrary zeros and one pole at origin, the PIDA controller can provide faster and smoother responses for the third-order plants than the PID controller [40,41]. In 2019, the PIDA was extended to the proportional-integral-derivative-accelerated-jerk (PIDAJ) controller for fourth-order plant [42]. In this

paper, the proposed MBA is applied to the control engineering application for designing the optimal 2DOF-PIDA controllers for the liquid-level system to archived input-tracking and load-regulating purposes. Results obtained by the 2DOF-PIDA controllers designed by the MBA will be compared with those obtained by the 1DOF-PID controller designed by Ziegler-Nichols (ZN) tuning rule [43,44], 2DOF-PID controllers designed by Araki-Taguchi (AT) tuning rule [6,9,45] and 1DOF-PID and 1DOF-PIDA controllers designed by MBA. This paper consists of six sections. After an introduction in Section 1, the concept of 2DOF control system is reviewed in Section 2. The proposed MBA algorithm is discussed in Section 3. Problem formulation of the MBA-based 2DOF-PIDA controllers design for the liquid-level system is performed in Section 4. Results and discussions are provided in Section 5. Finally, conclusions are given in Section 6.

2. **2DOF Control System.** Regarding to the 1DOF control system as shown in Figure 1, $P(s)$ is the transfer function model of the plant and $C(s)$ is the transfer function model of the controller, r is the reference input signal, e is the error signal, u is the control signal and d is the disturbance signal. From Figure 1, the closed-loop transfer functions from r to y and d to y are given in (1) and (2), respectively. Here, the subscript "1" means that the quantities are of the 1DOF control system.

$$G_{yr1}(s) = \frac{C(s)P(s)}{1 + C(s)P(s)} \tag{1}$$

$$G_{yd1}(s) = \frac{P(s)}{1 + C(s)P(s)} \tag{2}$$

$$G_{yr1}(s)P(s) + G_{yd1}(s) = P(s) \tag{3}$$

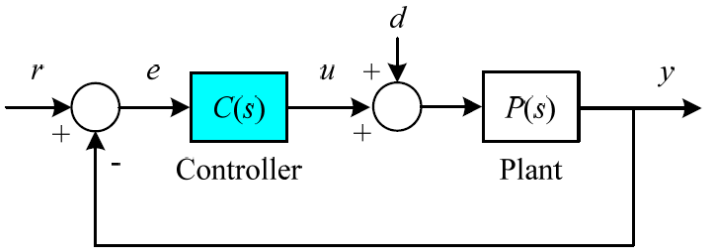

FIGURE 1. 1DOF control system

Those two transfer functions include only one controller $C(s)$. Therefore, they cannot be controlled independently. Such two functions in (1) and (2) are bound by (3). This means that based on two main purposes of control systems, their input-tracking and load-regulating responses cannot be independently controlled. From (3), it shows explicitly that for a given $P(s)$, $G_{yr1}(s)$ is uniquely determined if $G_{yd1}(s)$ is chosen, and vice versa. This fact causes the following difficulty. If the input-tracking response is optimized, the load-regulating response is often found to be poor, and vice versa. Effects between input-tracking and load-regulating responses of the 1DOF control system can be visualized from Figure 2.

A general structure of the 2DOF control system can be represented by the block diagram shown in Figure 3, where $C_f(s)$ is the transfer function model of the feedforward controller and $C(s)$ is the transfer function model of the main controller. From Figure 3, the closed-loop transfer functions from r to y and d to y are given in (4) and (5), respectively. The

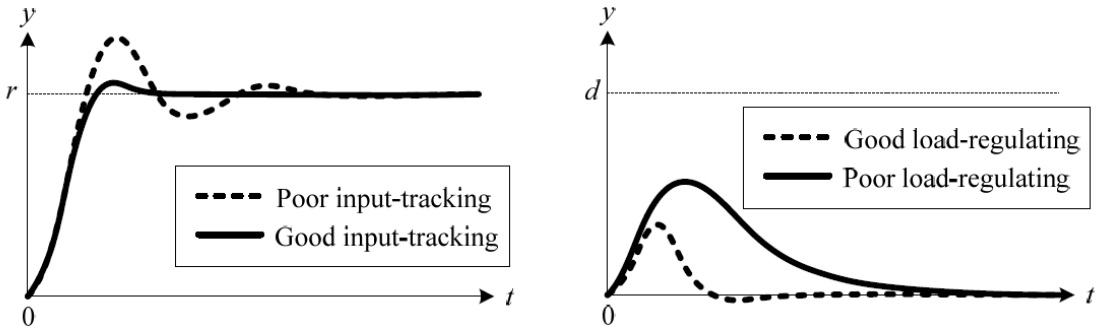

(a) Input-tracking responses (b) Load-regulating responses

FIGURE 2. Effects between input-tracking and load-regulating responses of the 1DOF control system

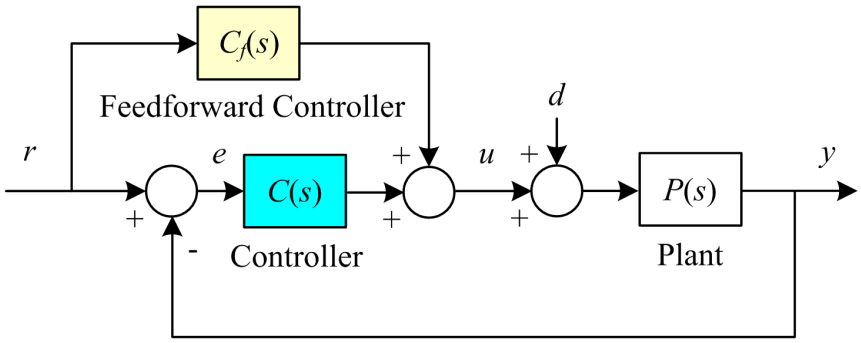

FIGURE 3. 2DOF control system

subscript "2" means that the quantities are of the 2DOF control system.

$$G_{yr2}(s) = \frac{[C(s) + C_f(s)]P(s)}{1 + C(s)P(s)} \tag{4}$$

$$G_{yd2}(s) = \frac{P(s)}{1 + C(s)P(s)} \tag{5}$$

By comparing (1)-(2) with (4)-(5), it was found that the closed-loop transfer functions of the 2DOF control system are related to those of the 1DOF control system as stated in (6)-(7). Once $C(s)$ is the same in both control systems, from (6)-(7), the load-regulating responses of 1DOF and 2DOF control systems are the same as shown in Figure 4(b), while the input-tracking responses differ by the amount of the second term of (6) which can be independently controlled by $C_f(s)$ as can be observed from Figure 4(a).

$$G_{yr2}(s) = G_{yr1}(s) + \frac{C_f(s)P(s)}{1 + C(s)P(s)} \tag{6}$$

$$G_{yd2}(s) = G_{yd1}(s) \tag{7}$$

Certainly, designing of the optimal 2DOF controller is more difficult than that of the optimal 1DOF controller. With this challenging task, the high efficient optimizer needs to be developed. Thus, the MBA is proposed in this paper. Algorithms of the original BA and the proposed MBA as well as their performance evaluation are presented in next section.

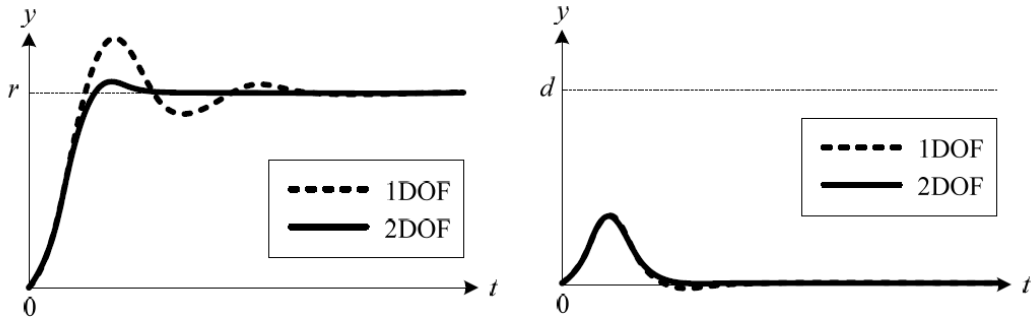

(a) Input-tracking responses (b) Load-regulating responses

FIGURE 4. Responses of 1DOF and 2DOF control systems

3. **Modified Bat Algorithm.** In this section, the original BA is briefly reviewed, the proposed MBA is elaborately described and the performance evaluation of the proposed MBA is investigated.

3.1. **Original BA.** Proposed by Yang [27], the BA's algorithm is based on the echolocation or bio-sonar characteristics of microbats which can formulate three following rules.

- All bats utilize echolocation to sense distance, and they also know the difference between food/prey and background barriers.
- Bats fly randomly with velocity $\boldsymbol{v}_i$ at position $\boldsymbol{x}_i$ with a frequency $f_{\min}$, varying wavelength λ and loudness $\boldsymbol{A}_0$ to search for prey. They automatically adjust the wavelength (or frequency) of their emitted pulses and adjust the rate of pulse emission $r \in [0, 1]$, depending on the proximity of their target.
- The loudness can vary from a large (positive) $\boldsymbol{A}_0$ to a minimum constant value $\boldsymbol{A}_{\min}$.

The BA's algorithm can be represented by the pseudo code as shown in Figure 5. In BA's algorithm, each bat is associated with a velocity $\boldsymbol{v}_i$ and a location $\boldsymbol{x}_i$, at iteration t, in a d-dimensional search space. Among all the bats, there exists a current best solution $\boldsymbol{x}^*$. Therefore, from above three rules, they can be translated into the updating equations for $\boldsymbol{x}_i$ and velocities $\boldsymbol{v}_i$ as stated in (8)-(10). When $\beta \in [0, 1]$ is a random vector drawn from a uniform distribution, each bat is randomly assigned a frequency which is drawn uniformly from $[f_{\min}, f_{\max}]$. Equation (8) represents the calculation of frequency f_i between $f_{\min}$ and $f_{\max}$ as the corresponding frequency boundaries. Equation (9) presents the calculation of a velocity $\boldsymbol{v}_i$ of each bat. Equation (10) stands for the calculation of a location $\boldsymbol{x}_i$ of each bat as the solutions. During the iterations, the loudness $\boldsymbol{A}_i$ and the pulse rates r_i are adjusted as expressed in (11) and (12) to balance the exploration and exploitation. From Equation (11), $0 < \alpha < 1$, the loudness $\boldsymbol{A}_i$ of each bat will be linearly decreased from $\boldsymbol{A}_i^t$ to zero as $t \to \infty$. From Equation (12), $\gamma > 0$, the pulse rates r_i of each bat will be logarithmically increased from r_i^t to r_i^0 as $t \to \infty$. According to Yang's recommendations, in the general case, users can use $\alpha = \gamma \in [0.9, 0.98]$ [27,28,31].

$$f_i = f_{\min} + (f_{\max} - f_{\min})\,\beta \tag{8}$$

$$\boldsymbol{v}_i^t = \boldsymbol{v}_i^{t-1} + \left(\boldsymbol{x}_i^{t-1} - \boldsymbol{x}^*\right) f_i \tag{9}$$

$$\boldsymbol{x}_i^t = \boldsymbol{x}_i^{t-1} + \boldsymbol{v}_i^t \tag{10}$$

$$\boldsymbol{A}_i^{t+1} = \alpha \boldsymbol{A}_i^t, \quad 0 < \alpha < 1 \tag{11}$$

$$r_i^{t+1} = r_i^0 \left(1 - e^{-\gamma t}\right), \quad \gamma > 0 \tag{12}$$

Objective function $f(\boldsymbol{x})$, $\boldsymbol{x} = (x_1,\ldots,x_d)^T$
Initialize the bat population $\boldsymbol{x}_i = (i = 1, 2,\ldots,n)$ and $\boldsymbol{v}_i$
Define pulse frequency f_i at $\boldsymbol{x}_i$
Initialize pulse rate r_i ($r_i = 0.5$ or 1.0 [27, 28, 31])
Initialize loudness $\boldsymbol{A}_i$ ($\boldsymbol{A}_i = 0.5$, 1.0 or 100 [27, 28, 31])
while ($t <$ Max_Iteration)
- Generate new solutions by adjusting frequency,
- Update velocities and locations/solutions
    if ($rand > r_i$)
        - Select as solution among the best solutions
        - Generate a local solution around the selected best solution
    end if
    - Generate a new solution by flying randomly
    if ($rand < \boldsymbol{A}_i \,\&\, f(\boldsymbol{x}_i) < f(\boldsymbol{x}^*)$)
        - Accept the new solutions
        - Increase r_i and reduce $\boldsymbol{A}_i$
    end if
- Rank the bats and find the current best $\boldsymbol{x}^*$
end while
Report the best solution found

FIGURE 5. Pseudo code of BA

3.2. **Proposed MBA.** In many cases especially in multi-modal optimization problems, the original BA is usually unable to escape from a local entrapment. To improve its performance, the new MBA is proposed in this paper as one of the modified versions of the original BA. The proposed MBA utilizes a random vector drawn from a Lévy-flight distribution which is more effective than the uniform distribution in order to increase the solution diversity. Therefore, a frequency used for each bat in (8) will be changed into (13), where a symbol Lévy(λ) represents a Lévy-flight distribution having an infinite variance with an infinite mean as expressed in (14). The step length s of calculation can be calculated by (15), where u and v stand for normal distribution as stated in (16), while standard deviations of u and v are also expressed in (17).

$$f_i = f_{\min} + (f_{\max} - f_{\min}) \times \text{Lévy}(\lambda) \tag{13}$$

$$\text{Lévy} \approx u = t^{-\lambda}, \quad (1 < \lambda \leq 3) \tag{14}$$

$$s = \frac{u}{|v|^{1/\beta}} \tag{15}$$

$$u \approx N(0,\ \sigma_u^2), \quad v \approx N(0,\ \sigma_v^2) \tag{16}$$

$$\sigma_u = \sqrt[\beta]{\frac{\Gamma(1+\beta)\sin(\pi\beta/2)}{\Gamma[(1+\beta)/2]\beta 2^{(\beta-1)/2}}}, \quad \sigma_v = 1 \tag{17}$$

In addition, to balance the exploration and exploitation of the proposed MBA, new loudness $\boldsymbol{A}_i$ and pulse rates r_i functions are proposed. From the original BA algorithm, during the iteration t, the loudness $\boldsymbol{A}_i$ will be decreased and the pulse rates r_i will be increased. The loudness $\boldsymbol{A}_i$ of the original BA in (11) is a linearly decreasing function. In the proposed MBA, three selected functions of the loudness $\boldsymbol{A}_i$ are stated in (18), (19) and (20), respectively, where $t_{\max}$ is the maximum iteration and t_x is the trigging iteration. From Equation (18), $0 < \alpha < 1$, the loudness $\boldsymbol{A}_i$ of each bat will be exponentially

decreased from $\boldsymbol{A}_0$ to zero, as $t = 0 \rightarrow t = t_{\max}$, plotted in Figure 6(a). From Equation (19), $\boldsymbol{A}_i$ of each bat will be logarithmically decreased from $\boldsymbol{A}_0$ to zero, as $t = 0 \rightarrow t = t_{\max}$, plotted in Figure 6(b). From Equation (20), $\boldsymbol{A}_i$ of each bat will be constant at $\boldsymbol{A}_0$ as $t = 0 \rightarrow t = t_x$, and linearly decreased from $\boldsymbol{A}_0$ to zero, as $t = t_x \rightarrow t = t_{\max}$, plotted in Figure 6(c).

$$\boldsymbol{A}_i^t = \boldsymbol{A}_0 e^{-\alpha t}, \quad 0 < \alpha < 1 \tag{18}$$

$$\boldsymbol{A}_i^t = \boldsymbol{A}_0 - e^{-\alpha(t_{\max} - t)}, \quad 0 < \alpha < 1 \tag{19}$$

$$\boldsymbol{A}_i^t = \begin{cases} \boldsymbol{A}_0, & 0 \le t < t_x \\ \alpha \boldsymbol{A}_i^t, & t_x \le t < t_{\max},\ 0 < \alpha < 1 \end{cases} \tag{20}$$

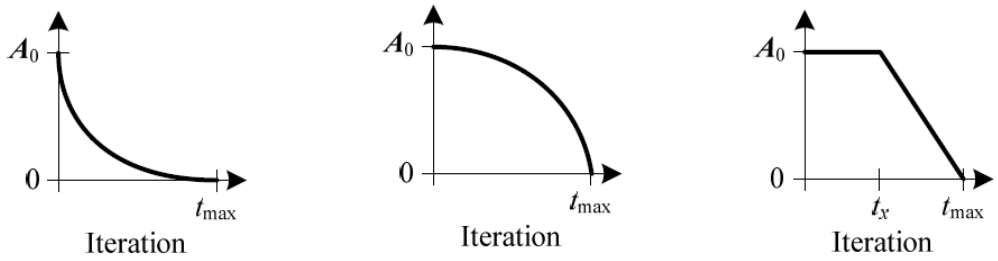

(a) Exponentially decreased

(b) Logarithmically decreased

(c) Constant-linearly decreased

FIGURE 6. Selected functions of loudness

The pulse rate r_i the original BA in (12) is a logarithmically increasing function. In the proposed MBA, three selected functions of the pulse rate r_i are expressed in (21), (22) and (23), respectively. From Equation (21), $0 < \gamma < 1$, the pulse rate r_i of each bat will be linearly increased from zero to r_0, as $t = 0 \rightarrow t = t_{\max}$, plotted in Figure 7(a). From Equation (22), r_i of each bat will be exponentially increased from zero to r_0, as $t = 0 \rightarrow t = t_{\max}$, plotted in Figure 7(b). From Equation (23), r_i of each bat will be constant at zero as $t = 0 \rightarrow t = t_x$, and linearly increased from zero to r_0, as $t = t_x \rightarrow t = t_{\max}$, plotted in Figure 7(c).

$$r_i^t = \gamma r_i^0, \quad 0 < \gamma < 1 \tag{21}$$

$$r_i^t = r_i^0 e^{-\gamma(t_{\max} - t)}, \quad 0 < \gamma < 1 \tag{22}$$

$$r_i^t = \begin{cases} 0, & 0 \le t < t_x \\ \gamma r_i^0, & t_x \le t < t_{\max},\ 0 < \gamma < 1 \end{cases} \tag{23}$$

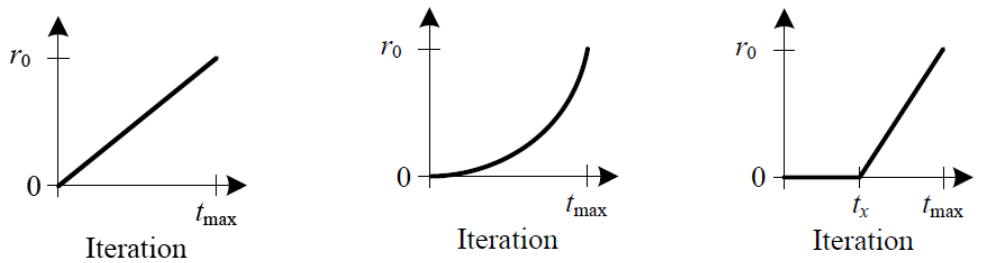

(a) Linearly increased

(b) Exponentially increased

(c) Constant-linearly increased

FIGURE 7. Selected functions of pulse rate

For preliminary studies, the proposed MBA was tested against several standard benchmark functions suggested by Jamil and Yang [46]. By varying α and γ with a Lévy-flight distribution, it was found that the best function of the loudness $\boldsymbol{A}_i$ is in (19), where $\alpha \in [0.8, 0.95]$, and the best function of the pulse rate r_i is in (22), where $\gamma \in [0.85, 0.98]$. From preliminary results, the convergent rates are not sensitive to the parameter variations. This means that the fine adjustment of algorithm-dependent parameters is not needed for any given problems. Therefore, the proposed MBA with a Lévy-flight distribution will use the loudness function in (19) with $\alpha = 0.85$ and the pulse rate function in (22) with $\gamma = 0.95$ for all applications in this work.

3.3. **Performance evaluation of MBA.** For comparison studies, the original BA and the proposed MBA are implemented by MATLAB version 2018a (License No.#40637337) run on Intel(R) Core(TM) i5-3470 CPU@3.60GHz, 4.0GB-RAM. Parameters of the original BA are set according to Yang's recommendations [27,28,31], i.e., the numbers of bats $n = 20$, the frequencies $f_{\min} = 0$, $f_{\max} = 2$, the loudness function in (11) with the initial loudness $\boldsymbol{A}_0 = 0.5$, the pulse rates function in (12) with the initial pulse rates $r_0 = 0.5$ and $\alpha = \gamma = 0.9$.

Parameters of the proposed MBA are set for a fair comparison as follows: $n = 20$, $f_{\min} = 0$, $f_{\max} = 2$, $\boldsymbol{A}_0 = 0.5$ in (19) with $\alpha = 0.85$, $r_0 = 0.5$ in (22) with $\gamma = 0.95$. 100 trials are conducted to find the best solutions. The algorithms stop when these two termination criteria (TC) are satisfied, i.e., (i) the variations of function values are less than a given tolerance $\varepsilon \leq 10^{-5}$ or (ii) the iteration reaches the maximum iteration (MaxIter = 1,000). The former criterion implies that the search is success, while the later means that the search is not success. Both BA and MBA are tested against 10 selected benchmark functions [46] as summarized in Table 1. For example, the 2D-surface of the Ackley function (f_1) is plotted in Figure 8.

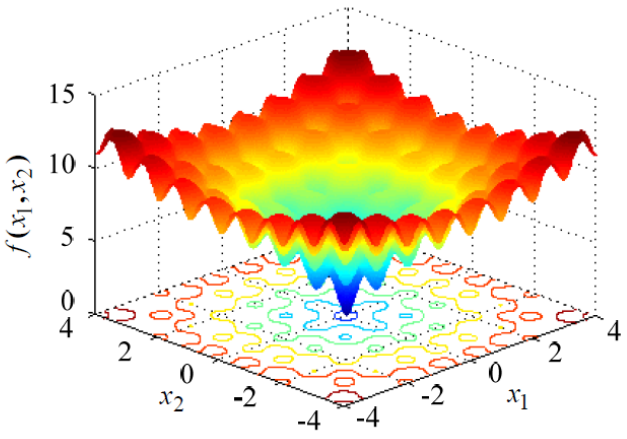

FIGURE 8. Ackley function surface

Results of comparison between BA and MBA are summarized in Table 2, where the numbers are in the format: average number (mean) of evaluations ± standard deviation (success rate). For instance, 3,067±1,632 (100%) means that the average number of function evaluations is 3,067 with the standard deviation of 1,632 and the success rate of 100%. The average number of function evaluations implies the searching time consumed. The less the average number of function evaluations, the less the searching time consumed. The standard deviation implies the robustness of the algorithm. The less the standard deviation, the more the robustness. From Table 2, the proposed MBA is much more

TABLE 1. Summary of selected test functions

Test functions	Names, Functions, Search spaces and Dimensions (D)	Optimal solutions ($\boldsymbol{x}^*$) Optimal function values $f(\boldsymbol{x}^*)$
f_1	Ackley function $f_1(\boldsymbol{x}) = -20e^{-0.02\sqrt{D^{-1}\sum_{i=1}^{D} x_i^2}} - e^{D^{-1}\sum_{i=1}^{D}\cos(2\pi x_i)} + 20 + e,$ $-35 \le x_i \le 35,\ D = 2$	$\boldsymbol{x}^* = (0, \ldots, 0),$ $f(\boldsymbol{x}^*) = 0$
f_2	Cosine mixture function $f_2(\boldsymbol{x}) = -0.1\sum_{i=1}^{D}\cos(5\pi x_i) - \sum_{i=1}^{D} x_i^2,$ $-1 \le x_i \le 1,\ D = 2$	$\boldsymbol{x}^* = (0, \ldots, 0),$ $f(\boldsymbol{x}^*) = 0.2$
f_3	Price–2 function $f_3(\boldsymbol{x}) = 1 + \sin^2 x_1 + \sin^2 x_2 - 0.1e^{-x_1^2 - x_2^3},$ $-10 \le x_i \le 10$	$\boldsymbol{x}^* = (0, 0),$ $f(\boldsymbol{x}^*) = 0.9$
f_4	Shubert–3 function $f_4(\boldsymbol{x}) = \sum_{i=1}^{D}\sum_{j=1}^{5} j\sin((j+1)x_i + j),$ $-10 \le x_i \le 10,\ D = 2$	$\boldsymbol{x}^* =$ multiple solutions, $f(\boldsymbol{x}^*) \approx -29.6733337$
f_5	Schaffer function $f_5(\boldsymbol{x}) = \sum_{i=1}^{D} 0.5 + \frac{\sin^2\sqrt{x_i^2 + x_{i+1}^2} - 0.5}{\left[1 + 0.001(x_i^2 + x_{i+1}^2)\right]^2},$ $-100 \le x_i \le 100,\ D = 2$	$\boldsymbol{x}^* = (0, \ldots, 0),$ $f(\boldsymbol{x}^*) = 0$
f_6	Bohachevsky–3 function $f_6(\boldsymbol{x}) = x_1^2 + 2x_2^2 - 0.3\cos(3\pi x_1 + 4\pi x_2) + 0.3,$ $-100 \le x_i \le 100$	$\boldsymbol{x}^* = (0, 0),$ $f(\boldsymbol{x}^*) = 0$
f_7	Easom function $f_7(\boldsymbol{x}) = -\cos(x_1)\cos(x_2)e^{[-(x_1-\pi)^2 - (x_2-\pi)^2]},$ $-100 \le x_i \le 100$	$\boldsymbol{x}^* = (\pi, \pi),$ $f(\boldsymbol{x}^*) = -1$
f_8	Keane function $f_8(\boldsymbol{x}) = \frac{\sin^2(x_1 - x_2)\sin^2(x_1 + x_2)}{\sqrt{x_1^2 + x_2^2}},$ $0 \le x_i \le 10$	$\boldsymbol{x}^* = \{(0, 1.39325), (1.39325, 0)\},$ $f(\boldsymbol{x}^*) = -0.673668$
f_9	Rosenbrock function $f_9(\boldsymbol{x}) = \sum_{i=1}^{D-1}[100(x_{i+1} - x_i^2)^2 + (x_i - 1)^2],$ $-30 \le x_i \le 30,\ D = 2$	$\boldsymbol{x}^* = (1, \ldots, 1),$ $f(\boldsymbol{x}^*) = 0$
f_{10}	Shubert Function $f_{10}(\boldsymbol{x}) = \prod_{i=1}^{D}\left(\sum_{j=1}^{5}\cos((j+1)x_i + j)\right),$ $-10 \le x_i \le 10,\ D = 2$	$\boldsymbol{x}^* = \{(-7.0835, 4.8580), (-7.0835, -7.7083), (-1.4251, -7.0835), (5.4828, 4.8580), (-1.4251, -0.8003), (4.8580, 5.4828), (-7.7083, -7.0835), (-7.0835, -1.4251), (-7.7083, -0.8003), (-7.7083, 5.4828), (-0.8003, -7.7083), (-0.8003, -1.4251), (-0.8003, 4.8580), (-1.4251, 5.4828), (5.4828, -7.7083), (4.8580, -7.0835), (5.4828, -1.4251), (4.8580, -0.8003)\},$ $f(\boldsymbol{x}^*) \approx -186.7309$

TABLE 2. Comparison results between BA and MBA

Test functions	Algorithms	
	BA	MBA
f_1	19,821±11,457(2%)	10,166±8,129(100%)
f_2	6,955±10,857(75%)	656±698(100%)
f_3	24,292±4,187(3%)	3,067±1,632(98%)
f_4	7,719±10,843(73%)	4,292±6,253(100%)
f_5	24,379±13,700(3%)	4,094±6,357(99%)
f_6	24,252±14,003(4%)	4,010±5,019(99%)
f_7	4,090±5,157(95%)	1,434±3,185(100%)
f_8	5,485±8,925(83%)	1,614±2,217(100%)
f_9	16,398±7,612(66%)	1,392±770(100%)
f_{10}	6,043±9,553(80%)	5,082±3,277(100%)

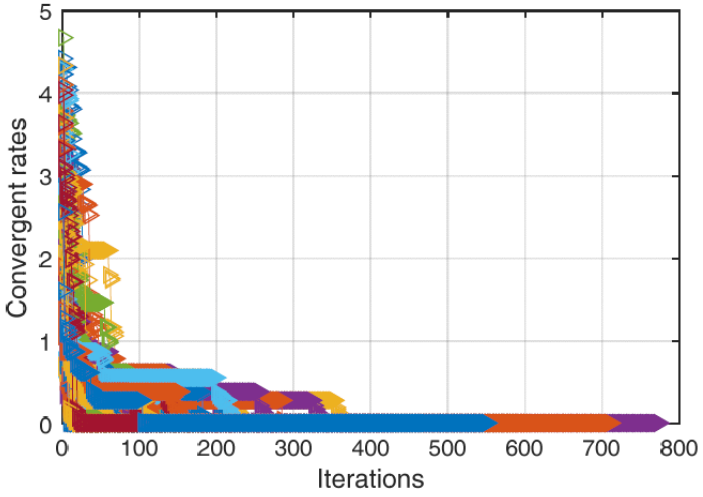

FIGURE 9. Convergent rates of Ackley function by MBA

efficient in finding the global optima of all selected benchmark functions with less average number of function evaluations, less standard deviation and higher success rates, than the original BA. With the less standard deviation, the proposed MBA provides more robustness of solution finding than the original BA, significantly. Figure 9 shows the convergent rates of optimal finding of Ackley function (f_1) by the proposed MBA as an example. It can be observed that the search of the MBA over f_1 is fully success (the success rate of 100%) and very high robustness. The convergent rates of other functions are omitted because they have a similar form to that of f_1 in Figure 9.

4. **Design Problem Formulation.** Problem formulation of the MBA-based 2DOF-PIDA controllers design for the liquid-level system is performed in this section. The mathematical model of the 3-tank liquid-level system is firstly formulated. Then, the optimization framework of the MBA-based 2DOF-PIDA controllers design for the 3-tank liquid-level system is given as follows.

4.1. **Mathematical model of liquid-level system.** The schematic diagram of the non-interaction 3-tank liquid-level system can be represented in Figure 10, where $q_i(t)$, $q_1(t)$ and $q_2(t)$ are liquid inflow rates into Tank-I, Tank-II and Tank-III, $q_o(t)$ is liquid outflow rate from Tank-III, $h_1(t)$, $h_2(t)$ and $h_3(t)$ are liquid levels of Tank-I, Tank-II and Tank-III,

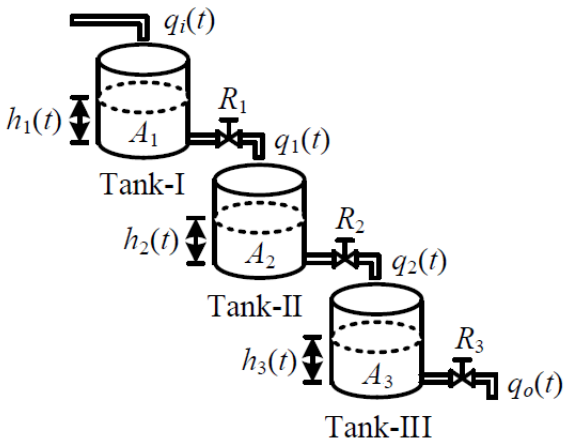

FIGURE 10. 3-tank liquid-level system

R_1, R_2 and R_3 are valve resistances of Tank-I, Tank-II and Tank-III, and A_1, A_2 and A_3 are capacitances (or cross-sectional areas) of Tank-I, Tank-II and Tank-III, respectively. In this work, the linearized mathematical model of the non-interaction 3-tank liquid-level system is formulated by setting $q_i(t)$ as input variable and $q_o(t)$ as output variable, respectively. Referring to Figure 10, linear differential equations of Tank-I, Tank-II and Tank-III are performed as stated in (24), (25) and (26), respectively. The transfer function of the non-interaction 3-tank liquid-level system is then formulated as expressed in (27), where $\tau_1 = R_1A_1$ is time constant of Tank-I, $\tau_2 = R_2A_2$ is time constant of Tank-II and $\tau_3 = R_3A_3$ is time constant of Tank-III, respectively.

$$q_i(t) - q_1(t) = A_1\frac{dh_1(t)}{dt}, \quad q_1(t) = \frac{h_1(t)}{R_1} \tag{24}$$

$$q_1(t) - q_2(t) = A_2\frac{dh_2(t)}{dt}, \quad q_2(t) = \frac{h_2(t)}{R_2} \tag{25}$$

$$q_2(t) - q_o(t) = A_3\frac{dh_3(t)}{dt}, \quad q_o(t) = \frac{h_3(t)}{R_3} \tag{26}$$

$$\begin{aligned} P(s) = \frac{Q_o(s)}{Q_i(s)} &= \frac{1}{(R_1A_1s+1)(R_2A_2s+1)(R_3A_3s+1)} \\ &= \frac{1}{(\tau_1s+1)(\tau_2s+1)(\tau_3s+1)} \end{aligned} \tag{27}$$

Once setting $\tau_1 = 1$ s, $\tau_2 = 1/2$ s and $\tau_3 = 1/3$ s as appearing in [47], the overall transfer function of the 3-tank liquid-level system can be rewritten in (28). The model expressed in (28) will be used as a plant in the considered control system design optimization approach.

$$P(s) = \frac{6}{(s+1)(s+2)(s+3)} \tag{28}$$

4.2. **MBA-based 2DOF-PIDA controllers design.** Referring to Figure 3, the MBA-based 2DOF-PIDA controllers design for the 3-tank liquid-level system can be represented by the block diagram as shown in Figure 11. The main controller $C(s)$ and the feedforward controller $F(s)$ are defined to be the PIDA controllers as expressed in (29) and (30) [40], where K_p is proportional gain, K_i is integral gain, K_d is derivative gain and K_a is

accelerated gain, respectively.

$$C(s)|_{PIDA} = K_{p,c} + \frac{K_{i,c}}{s} + K_{d,c}s + K_{a,c}s^2 \tag{29}$$

$$F(s)|_{PIDA} = K_{p,f} + \frac{K_{i,f}}{s} + K_{d,f}s + K_{a,f}s^2 \tag{30}$$

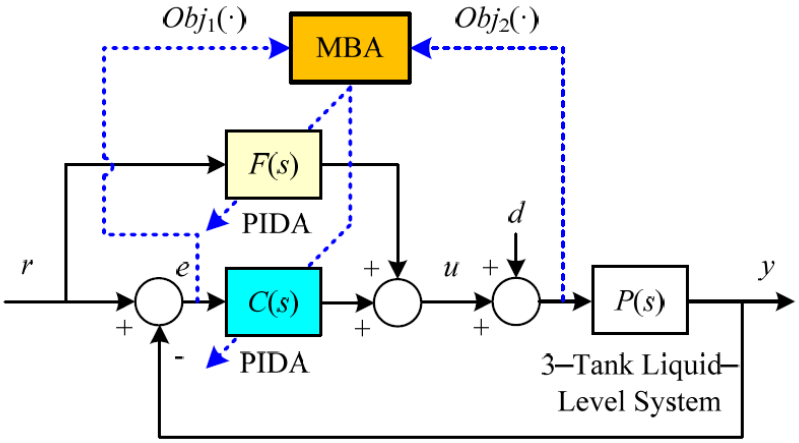

FIGURE 11. MBA-based 2DOF-PIDA controllers design

For the MBA-based 2DOF-PIDA design optimization framework in Figure 11, the input-tracking and load-regulating responses are set as two particular objective functions, i.e., $Obj_1(\cdot)$ = input-tracking response and $Obj_2(\cdot)$ = load-regulating response. In this work, both $Obj_1(\cdot)$ and $Obj_2(\cdot)$ are combined to be the main objective function $\boldsymbol{J}(\cdot)$ by using the penalty factors with normalization as stated in (31) where α_1 and α_2 are the penalty factors, while Obj_{1_Max} and Obj_{2_Max} are the maximum values of $Obj_1(\cdot)$ and $Obj_2(\cdot)$, respectively. The penalty factors, $0 \le \alpha_1, \alpha_2 \le 1$, are arbitrary set by users. In some works emphasizing the input-tracking response improvement, the value of α_1 should be more than that of α_2. On the other hand, if the load-regulating response needs to be mainly improved, the value of α_2 should be more than that of α_1. However, $\alpha_1 = 0.5$ and $\alpha_2 = 0.5$ are set in this work because both the input-tracking and load-regulating responses are considered as the same essence of control purposes.

$$\textbf{Min } \boldsymbol{J}(\cdot) = \alpha_1 \left(\frac{Obj_1(\cdot)}{Obj_{1\_\mathrm{Max}}} \right) + \alpha_2 \left(\frac{Obj_2(\cdot)}{Obj_{2\_\mathrm{Max}}} \right) \tag{31}$$

$$\left.\begin{aligned} \text{Subject to } \; & t_r \le t_{r\_\max},\ M_p \le M_{p\_\max},\ t_s \le t_{s\_\max}, \\ & E_{ss} \le E_{ss\_\max},\ M_{preg} \le M_{preg\_\max},\ t_{reg} \le t_{reg\_\max}, \\ & K_{p,c\_\min} \le K_{p,c} \le K_{p,c\_\max},\ K_{i,c\_\min} \le K_{i,c} \le K_{i,c\_\max}, \\ & K_{d,c\_\min} \le K_{d,c} \le K_{d,c\_\max},\ K_{a,c\_\min} \le K_{a,c} \le K_{a,c\_\max}, \\ & K_{p,f\_\min} \le K_{p,f} \le K_{p,f\_\max},\ K_{i,f\_\min} \le K_{i,f} \le K_{i,f\_\max}, \\ & K_{d,f\_\min} \le K_{d,f} \le K_{d,f\_\max},\ K_{a,f\_\min} \le K_{a,f} \le K_{a,f\_\max} \end{aligned}\right\} \tag{32}$$

From (31), $\boldsymbol{J}(\cdot)$ including $Obj_1(\cdot)$ and $Obj_2(\cdot)$ will be fed to the MBA as shown in Figure 11 to be minimized by searching for optimal parameters of two PIDA controllers, $C(s)$ and $F(s)$ in (29) and (30), corresponding to their constraints and search spaces defined as expressed in (32), where t_r is rise time, $t_{r\_\max}$ is maximum allowance of t_r, M_p is overshoot, $M_{p\_\max}$ is maximum allowance of M_p, t_s is settling time, $t_{s\_\max}$ is maximum allowance of t_s, E_{ss} is steady-state error, $E_{ss\_\max}$ is maximum allowance of E_{ss}, M_{preg} is overshoot from regulation, $M_{preg\_\max}$ is maximum allowance of M_{preg}, t_{reg} is regulation

time, $t_{reg\_\max}$ is maximum allowance of t_{reg}, $K_{p,c\_\min}$ is lower bound of gain $K_{p,c}$, $K_{p,c\_\max}$ is upper bound of gain $K_{p,c}$, $K_{i,c\_\min}$ is lower bound of gain $K_{i,c}$, $K_{i,c\_\max}$ is upper bound of gain $K_{i,c}$, $K_{d,c\_\min}$ is lower bound of gain $K_{d,c}$, $K_{d,c\_\max}$ is upper bound of gain $K_{d,c}$, $K_{a,c\_\min}$ is lower bound of gain $K_{a,c}$, $K_{a,c\_\max}$ is upper bound of gain $K_{a,c}$, $K_{p,f\_\min}$ is lower bound of gain $K_{p,f}$, $K_{p,f\_\max}$ is upper bound of gain $K_{p,f}$, $K_{i,f\_\min}$ is lower bound of gain $K_{i,f}$, $K_{i,f\_\max}$ is upper bound of gain $K_{i,f}$, $K_{d,f\_\min}$ is lower bound of gain $K_{d,f}$, $K_{d,f\_\max}$ is upper bound of gain $K_{d,f}$, $K_{a,f\_\min}$ is lower bound of gain $K_{a,f}$ and $K_{a,f\_\max}$ is upper bound of gain $K_{a,f}$.

5. **Results and Discussions.** For design comparison, results of the 3-tank liquid-level controlled system with the 1DOF-PID controller designed by ZN tuning rule, 2DOF-PID controllers designed by AT tuning rule, 1DOF-PID, 1DOF-PIDA and 2DOF-PIDA controllers designed by MBA are consecutively presented.

5.1. **1DOF-PID controller designed by ZN.** For the first method of ZN tuning rule [43,44], the open-loop step response of $P(s)$ in (28) provides the S-shape process reaction curve having delay time $L = 0.4211$ s and time constant $T = 2.3157$ s. Referring to Figure 1 and Table 3, the 1DOF-PID controller parameters can be calculated as follows: K_c (controller gain) $= 1.2T/L = 6.599$, τ_i (integral time constant) $= 2L = 0.8422$ s and τ_d (derivative time constant) $= 0.5L = 0.2105$ s. Therefore, the 1DOF-PID controller designed by the ZN tuning rule for the 3-tank liquid-level system is expressed in (33).

$$C(s)|_{1DOF\text{-}PID\text{-}ZN} = K_c\left(1 + \frac{1}{\tau_i s} + \tau_d s\right) = K_p + \frac{K_i}{s} + K_d s = 6.60 + \frac{7.84}{s} + 1.39s \quad (33)$$

Table 3. ZN tuning rule based on delay time L and time constant T

Controllers	Parameters		
	K_c	τ_i	τ_d
P	T/L	∞	0
PI	$0.9T/L$	$L/0.3$	0
PID	$1.2T/L$	$2L$	$0.5L$

The input-tracking responses of the 3-tank liquid-level system without and with the 1DOF-PID controller designed by the ZN tuning rule are plotted in Figure 12(a), while the load-regulating response of the 3-tank liquid-level controlled system with the 1DOF-PID controller designed by the ZN tuning rule is depicted in Figure 12(b). From Figure 12(a), the input-tracking response of the 3-tank liquid-level system without controller yields $t_r = 2.73$ s, $M_p = 0\%$, $t_s = 5.00$ s and $E_{ss} = 0\%$, while that of the 3-tank liquid-level system with the 1DOF-PID controller designed by the ZN tuning rule gives $t_r = 0.63$ s, $M_p = 54.14\%$, $t_s = 6.97$ s and $E_{ss} = 0\%$. From Figure 12(b), the 3-tank liquid-level controlled system with the 1DOF-PID controller designed by the ZN tuning rule can regulate the step load disturbance. It yields the maximum percent overshoot from load disturbance regulation $M_{preg} = 14.59\%$ and the regulating time $t_{reg} = 7.50$ s.

5.2. **2DOF-PID controller designed by AT.** Referring to Figure 3, $C(s)$ and $C_f(s)$ of the 2DOF-PID controllers according to the AT tuning rule are defined as stated in (34) and (35) [6,9,45].

$$C(s)|_{2DOF\text{-}PID\text{-}AT} = K_c\left(1 + \frac{1}{\tau_i s} + \tau_d s\right) \quad (34)$$

$$C_f(s)|_{2DOF\text{-}PID\text{-}AT} = -K_c(\alpha + \beta\tau_d s) \quad (35)$$

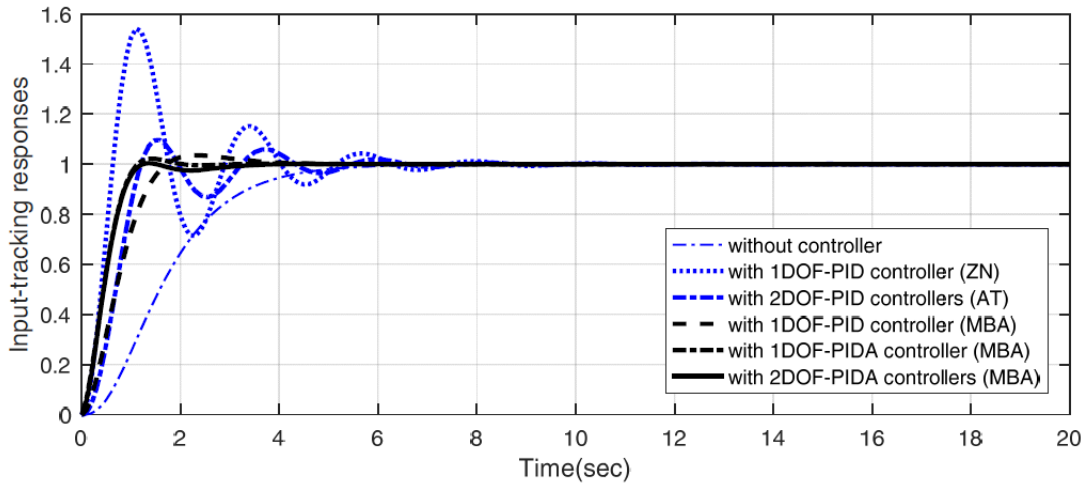

(a) Input-tracking responses

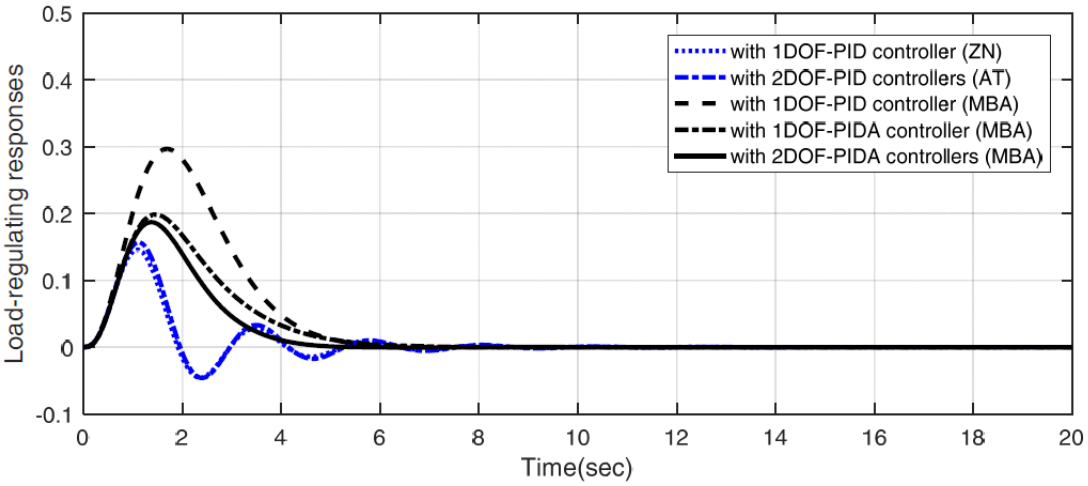

(b) Load-regulating responses

FIGURE 12. (color online) Responses of the 3-tank liquid-level system without and with 1DOF-PID, 2DOF-PID, 1DOF-PIDA and 2DOF-PIDA controllers

Regarding to the S-shape process reaction curve giving $L = 0.4211$ s and $T = 2.3157$ s, the ratio of $L/T \approx 0.2$. From the AT tuning rule [6,9,10,45] as summarized in Table 4, the 2DOF-PID parameters can be determined as follows: $K_c = 6.32$, $\tau_i = 0.4T = 0.9263$ s, $\tau_d = 0.08T = 0.1853$ s, $\alpha = 0.61$ and $\beta = 0.64$. Therefore, the 2DOF-PID controllers designed by the AT tuning rule for the 3-tank liquid-level system are given in (36) and (37).

$$C(s)|_{2DOF\text{-}PID\text{-}AT} = 6.32 + \frac{6.82}{s} + 1.17s \tag{36}$$

$$C_f(s)|_{2DOF\text{-}PID\text{-}AT} = -3.86 - 0.75s \tag{37}$$

The input-tracking responses of the 3-tank liquid-level system without and with the 2DOF-PID controllers designed by the AT tuning rule are plotted in Figure 12(a), while the load-regulating response of the 3-tank liquid-level controlled system with the 2DOF-PID controllers designed by the AT tuning rule is depicted in Figure 12(b). Referring to Figure 12(a), the input-tracking response of the 3-tank liquid-level controlled system with

TABLE 4. AT tuning rule of 2DOF-PID controllers based on delay time L and time constant T

Ratio L/T	2DOF-PID parameters				
	K_c	τ_i/T	τ_d/T	α	β
0.1	12.57	0.22	0.04	0.64	0.66
0.2	6.32	0.40	0.08	0.61	0.64
0.4	3.21	0.69	0.16	0.56	0.61
0.8	1.68	1.09	0.30	0.47	0.54

the 2DOF-PID controllers designed by the AT tuning rule gives $t_r = 1.20$ s, $M_p = 9.61\%$, $t_s = 5.19$ s and $E_{ss} = 0\%$. From Figure 12(b), the 3-tank liquid-level controlled system with the 2DOF-PID controllers designed by the AT tuning rule can regulate the step load disturbance. It provides $M_{preg} = 15.67\%$ and the regulating time $t_{reg} = 8.12$ s.

5.3. **1DOF-PID controller designed by MBA.** Referring to Figure 11 in order to design an optimal 1DOF-PID controller for the 3-tank liquid-level system by the proposed MBA, the algorithm of the MBA is coded by MATLAB. The search parameters of the MBA are defined as appearing in subsection 3.3. MaxIter = 500 is then set as the TC. 50 trials are conducted to find the best solutions (optimal 1DOF-PID controller for the 3-tank liquid-level system). Search spaces and their constraint functions are then performed as shown in (38). For the 1DOF-PID controller design, $F(s)$ in Figure 11 is removed.

$$\left.\begin{array}{ll}\text{Subject to} & t_r \le 2.0 \text{ s},\ M_p \le 5.0\%,\ t_s \le 5.0 \text{ s},\\ & E_{ss} \le 0.01\%,\ M_{preg} \le 30\%,\ t_{reg} \le 8.0 \text{ s},\\ & 0 \le K_p \le 5.0,\ 0 \le K_i \le 5.0,\ 0 \le K_d \le 2.5\end{array}\right\} \tag{38}$$

$$C(s)|_{1DOF\text{-}PID\text{-}MBA} = 2.10 + \frac{1.46}{s} + 0.75s \tag{39}$$

After the search process stopped, the MBA can successfully provide the optimal parameters of the 1DOF-PID controller of the 3-tank liquid-level system as stated in (39). The input-tracking responses of the 3-tank liquid-level system without and with the 1DOF-PID controller designed by the MBA are plotted in Figure 12(a), while the load-regulating response with the 1DOF-PID controller designed by the MBA is depicted in Figure 12(b). Referring to Figure 12(a), the input-tracking response of the 3-tank liquid-level controlled system with the 1DOF-PID controller designed by the MBA yields $t_r = 1.71$ s, $M_p = 3.57\%$, $t_s = 3.12$ s and $E_{ss} = 0\%$. From Figure 12(b), the 3-tank liquid-level controlled system with the 1DOF-PID controller designed by the MBA can regulate the step load disturbance. It provides $M_{preg} = 29.65\%$ and the regulating time $t_{reg} = 7.02$ s.

5.4. **1DOF-PIDA controller designed by MBA.** To design an optimal 1DOF-PIDA controller for the 3-tank liquid-level system by the MBA, search spaces and their constraint functions are then performed as stated in (40). In this case, $F(s)$ in Figure 11 is also removed. Once the search process stopped, the MBA can successfully provide the optimal parameters of the 1DOF-PIDA controller as expressed in (41). The input-tracking responses of the 3-tank liquid-level system without and with the 1DOF-PIDA controller designed by the MBA are plotted in Figure 12(a), while the load-regulating response with the 1DOF-PIDA controller is depicted in Figure 12(b).

$$\left.\begin{array}{ll}\text{Subject to} & t_r \le 2.0 \text{ s},\ M_p \le 5.0\%,\ t_s \le 5.0 \text{ s},\\ & E_{ss} \le 0.01\%,\ M_{preg} \le 30\%,\ t_{reg} \le 8.0 \text{ s},\\ & 0 \le K_p \le 5.0,\ 0 \le K_i \le 5.0,\ 0 \le K_d \le 2.5,\ 0 \le K_a \le 0.5\end{array}\right\} \tag{40}$$

$$C(s)|_{1DOF\text{-}PIDA\text{-}MBA} = 3.60 + \frac{2.20}{s} + 1.60s + 0.06s^2 \tag{41}$$

From Figure 12(a), the input-tracking response of the 3-tank liquid-level controlled system with the 1DOF-PIDA controller designed by the MBA gives $t_r = 1.13$ s, $M_p = 2.22\%$, $t_s = 1.53$ s and $E_{ss} = 0\%$. From Figure 12(b), the 3-tank liquid-level controlled system with the 1DOF-PIDA controller designed by the MBA can regulate the step load disturbance. It provides $M_{preg} = 19.82\%$ and the regulating time $t_{reg} = 7.05$ s.

5.5. **2DOF-PIDA controller designed by MBA.** Finally, in order to design the optimal 2DOF-PIDA controllers for the 3-tank liquid-level system by the MBA, search spaces and their constraint functions are then performed as stated in (42). The MBA can successfully provide the optimal parameters of the 2DOF-PIDA controllers as expressed in (43) and (44). The input-tracking and the load-regulating responses of the 3-tank liquid-level control system are depicted in Figure 12(a) and Figure 12(b), respectively.

$$\left.\begin{array}{ll} \text{Subject to} & t_r \le 2.0 \text{ s},\ M_p \le 5.0\%,\ t_s \le 5.0 \text{ s},\ E_{ss} \le 0.01\%, \\ & M_{preg} \le 30\%,\ t_{reg} \le 8.0 \text{ s},\ 0 \le K_{p,c} \le 5.0,\ 0 \le K_{i,c} \le 10, \\ & 0 \le K_{d,c} \le 2.0,\ 0 \le K_{a,c} \le 0.5,\ -1.0 \le K_{p,f} \le 1.0, \\ & -1.0 \le K_{i,f} \le 1.0,\ -1.0 \le K_{d,f} \le 1.0,\ -1.0 \le K_{a,f} \le 1.0 \end{array}\right\} \tag{42}$$

$$C(s)|_{2DOF\text{-}PIDA\text{-}MBA} = 3.95 + \frac{2.85}{s} + 1.61s + 0.06s^2 \tag{43}$$

$$F(s)|_{2DOF\text{-}PIDA\text{-}MBA} = -0.45 + \frac{0.0013}{s} - 0.05s + 0.0012s^2 \tag{44}$$

From Figure 12(a), the input-tracking response of the 3-tank liquid-level controlled system with the 2DOF-PIDA controllers designed by the MBA yields $t_r = 1.21$ s, $M_p = 0.65\%$, $t_s = 2.58$ s and $E_{ss} = 0\%$. From Figure 12(b), the 3-tank liquid-level controlled system with the 2DOF-PIDA controllers designed by the MBA can completely regulate the step load disturbance. It gives $M_{preg} = 18.73\%$ and the regulating time $t_{reg} = 4.82$ s.

For comparison of all systems from Figure 12(a) and Figure 12(b), it was found that the 3-tank liquid-level controlled systems with the 1DOF-PID, 2DOF-PID, 1DOF-PIDA and 2DOF-PIDA controllers are stable and can regulate the step load disturbance. However, the 2DOF-PIDA controllers designed by the MBA can provide faster and smoother outflow rate response than other controllers. As results, the advantages of the 2DOF control system over the 1DOF are confirmed, and the performance of the proposed MAB for the considered control design application is verified.

6. **Conclusions.** An optimal design of the 2DOF-PIDA controllers for the liquid-level system by using the MBA has been proposed in this paper. The proposed MBA is the new modified version of the original BA developed to improve its exploration and exploitation properties. By utilizing the random number drawn from a Lévy-flight distribution and new loudness and pulse emission rate functions, simulation results have shown that the proposed MBA is much more efficient in finding the global optimum than the original BA. The MBA has been applied to designing the optimal 2DOF-PIDA controllers for the 3-tank liquid-level system to achieve two main purposes of control systems. As results, the 3-tank liquid-level controlled system with the 2DOF-PIDA controllers designed by the MBA could provide very satisfactory responses superior to those with the 1DOF-PID designed by ZN tuning rule, 2DOF-PID designed by AT tuning rule, 1DOF-PID and 1DOF-PIDA designed by MBA, respectively. For future research, the proposed MBA-based 2DOF-PIDA design optimization framework will be extended to various control engineering problems.

REFERENCES

[1] K. Ogata, *Modern Control Engineering*, 5th Edition, Pearson Prentice Hall, 2010.
[2] B. C. Kuo and F. Golnaraghi, *Automatic Control Systems*, 9th Edition, John Wiley & Sons, 2010.
[3] R. C. Dorf and R. H. Bishop, *Modern Control Systems*, 13th Edition, Pearson Prentice Hall, 2017.
[4] I. M. Horowitz, *Synthesis of Feedback Systems*, Academic Press, 1963.
[5] K. J. Åström and T. Hägglund, *Advanced PID Control*, ISA Press, 2006.
[6] M. Araki and H. Taguchi, Two-degree-of-freedom PID controllers, *International Journal of Control, Automation, and Systems*, vol.1, no.4, pp.401-411, 2003.
[7] M. Araki, PID control system with reference feedforward (PID-FF control system), *Proc. of the 23rd SICE (Society of Instrument and Control Engineers) Annual Conference*, pp.31-32, 1984.
[8] M. Araki, On two-degree-of-freedom PID control systems, *SICE Research Committee on Modeling and Control Design of Real Systems*, 1984.
[9] M. Araki, Two-degree-of-freedom control system: Part I, *Systems and Control*, vol.29, pp.649-656, 1985.
[10] K. Hiroi, Two-degree-of-freedom PID control system and its application, *Instrumentation*, vol.29, pp.39-43, 1986.
[11] M. Namie, T. Ueda, T. Tsukabe and H. Taguchi, Two-degree-of-freedom PID controller used for temperature control: Simultaneity reference response and disturbance response, *OMRON Technics*, vol.28, pp.285-291, 1988.
[12] K. Hiroi and K. Yonezawa, Reference-filter type two-degree-of-freedom PID control system, *Proc. of the 24th SICE (Society of Instrument and Control Engineers) Annual Conference*, pp.217-218, 1985.
[13] K. Hiroi and Y. Yamamoto, Component-separated type two-degree-of-freedom PID control system, *Proc. of the 24th SICE (Society of Instrument and Control Engineers) Annual Conference*, pp.219-220, 1985.
[14] H. Taguchi, M. Doi and M. Araki, Optimal parameters of two-degree-of-freedom PID control systems, *Trans. SICE*, vol.23, pp.889-895, 1987.
[15] K. Hiroi and K. Nagakawa, Improvement of a digital PID algorithm with rate limitation on MV change, *Proc. of the 28th SICE (Society of Instrument and Control Engineers) Annual Conference*, pp.243-244, 1989.
[16] K. Hiroi, A. Nomura, A. Yoneya and Y. Togari, Advanced two-degree-of-freedom PID algorithm, *Proc. of the 29th SICE (Society of Instrument and Control Engineers) Annual Conference*, pp.49-50, 1990.
[17] M. Kanda and K. Hiroi, Super two-degree-of-freedom PID algorithm, *Proc. of the 30th SICE (Society of Instrument and Control Engineers) Annual Conference*, pp.465-466, 1991.
[18] S. Yamazaki and K. Hiroi, Application of reference-filter type 2DOF PID to boiler control, *Instrumentation*, vol.30, pp.114-119, 1987.
[19] V. Zakian, *Control Systems Design: A New Framework*, Springer-Verlag, 2005.
[20] D. H. Kim, Tuning of 2-DOF PID controller by immune algorithm, *Proc. of the CEC'02 Congress on Evolutionary Computational*, pp.675-680, 2002.
[21] T. Kawabe, Robust 2DOF PID controller design of time-delay systems based on evolutionary computation, *Proc. of the 4th WSEAS International Conference on Electronics, Control and Signal Processing*, pp.144-149, 2005.
[22] H. Nemati and P. Bagheri, A new approach to tune two degree of freedom (2DOF) PI controller, *Proc. of the IEEE Multi-Conference on Systems and Control*, pp.1819-1824, 2010.
[23] K. Latha and V. Rajinikanth, 2DOF PID controller tuning for unstable systems using bacterial foraging algorithm, *Proc. of the 3rd International Conference on Swarm, Evolutionary, and Memetic Computing*, pp.519-527, 2012.
[24] P. Dash, L. C. Saikia and N. Sinha, Comparison of performances of several cuckoo search algorithm based 2DOF controllers in AGC of multi-area thermal system, *Electrical Power and Energy Systems*, vol.55, pp.429-436, 2014.
[25] R. F. Hassan, Design and implementation of two degree of freedom proportional integral derivative controller, *Proc. of the 7th International Conference on Information Technology*, pp.75-80, 2015.
[26] D. Puangdownreong, D. Kumpanya, C. Kiree and S. Tunyasrirut, Optimal tuning of 2DOF-PID controllers of BLDC motor speed control system by intensified current search, *Proc. of the 2015 Global Engineering & Applied Science Conference*, pp.107-115, 2015.
[27] X. S. Yang, A new metheuristic bat-inspired algorithm, *Nature Inspired Cooperative Strategies for Optimization*, vol.284, pp.65-74, 2012.

[28] X. S. Yang, Bat algorithm for multiobjective optimization, *International Journal of Bio-Inspired Computation*, vol.3, no.5, pp.267-274, 2011.
[29] C. Thammarat, K. Lurang, D. Puangdownreong, S. Suwammarongsri, S. Hlangnamthip and A. Nawikavatan, Application of bat-inspired algorithm to optimal PIDA controller design for liquid-level system, *Proc. of the iEECON2018 International Conference*, pp.556-559, 2018.
[30] K. Lurang, C. Thammarat, S. Hlangnamthip and D. Puangdownreong, Optimal design of two-degree-of-freedom PIDA controllers for liquid-level system by bat-inspired algorithm, *International Journal of Circuits, Systems and Signal Processing*, vol.13, pp.34-39, 2019.
[31] X. S. Yang and X. He, Bat algorithm: Literature review and applications, *International Journal of Bio-Inspired Computation*, vol.5, no.3, pp.141-149, 2013.
[32] K. Khan, A. Nikov and A. Sahai, A fuzzy bat clustering method for ergonomic screening of office workplaces, *Advances in Intelligent and Soft Computing*, vol.101, no.1, pp.59-66, 2011.
[33] G. Komarasamy and A. Wahi, An optimized K-means clustering technique using bat algorithm, *European Journal of Scientific Research*, vol.84, no.2, pp.263-273, 2012.
[34] J. H. Lin, C. W. Chou, C. H. Yang and H. L. Tsai, A chaotic Lévy fight bat algorithm for parameter estimation in nonlinear dynamic biological systems, *Journal of Computer and Information Technology*, vol.2, no.2, pp.56-63, 2012.
[35] R. Y. M. Nakamura, L. A. M. Pereira, K. A. Costa, D. Rodrigues, J. P. Papa and X. S. Yang, BBA: A binary bat algorithm for feature selection, *Proc. of the 25th IEEE SIBGRAPI Conference on Graphics, Patterns and Images (SIBGRAPI)*, pp.291-297, 2012.
[36] J. Xie, Y. Q. Zhou and H. Chen, A novel bat algorithm based on differential operator and Lévy fights trajectory, *Computational Intelligence and Neuroscience*, vol.2013, 2013.
[37] J. W. Zhang and G. G. Wang, Image matching using a bat algorithm with mutation, *Applied Mechanics and Materials*, vol.203, no.1, pp.88-93, 2012.
[38] G. Wang and L. Guo, A novel hybrid bat algorithm with harmony search for global numerical optimization, *Journal of Applied Mathematics*, vol.2013, 2013.
[39] Z. Haruna, M. B. Múazu, K. A. Abubilal and S. A. Tijani, Development of a modified bat algorithm using elite opposition-based learning, *Proc. of the IEEE 3rd International Conference on Electro-Technology for National Development (NIGERCON)*, pp.144-151, 2017.
[40] S. Jung and R. C. Dorf, Analytic PIDA controller design technique for a third order system, *Proc. of the 35th IEEE Conference on Decision and Control*, pp.2513-2518, 1996.
[41] P. Pannil, T. Sungsorn, T. Trisuwannawat and P. Ukakimaparn, Design of discrete-time PIDA controller using Kitti's method with first-order hold discretization, *ICIC Express Letters*, vol.12, no.6, pp.567-574, 2018.
[42] P. Ukakimaparn, K. Tirasesth, T. Trisuwannawat and P. Pannil, Closed-form formulas for continuous/discrete-time PIDAJ controller's parameters, *ICIC Express Letters*, vol.13, no.7, pp.645-652, 2019.
[43] J. G. Ziegler and N. B. Nichols, Optimum settings for automatic controllers, *Transactions on ASME*, vol.64, pp.759-768, 1942.
[44] J. G. Ziegler and N. B. Nichols, Process lags in automatic control circuits, *Transactions on ASME*, vol.65, pp.433-444, 1943.
[45] H. Taguchi and M. Araki, Two-degree-of-freedom PID controllers: Their functions and optimal tuning, *Proc. of the IFAC Workshop on Digital Control: Past, Present and Future of PID Control*, pp.91-96, 2000.
[46] M. Jamil and X. S. Yang, A literature survey of benchmark functions for global optimization problems, *International Journal of Mathematical Modelling and Numerical Optimisation*, vol.4, no.2, pp.150-194, 2013.
[47] P. Srinivas, K. V. Lakshmi and V. N. Kumar, A comparison of PID controller tuning methods for three tank level process, *International Journal of Advanced Research in Electrical, Electronics and Instrumentation Engineering*, vol.3, no.1, pp.6810-6820, 2014.